

Supplementary Information

Exploring Redox Activity in $\text{LiCoPO}_4 - \text{LiCo}_2\text{P}_3\text{O}_{10}$ Tailored Positive Electrode for 5V Lithium Ion Batteries: Rigid Band Behavior of Electronic Structure and Stability of Delithiated Phase.

Gennady Cherkashinin,^{*,a} Mikhail V. Lebedev,^b Sankaramangalam Ulhas Sharath,^a Andreas Hajduk,^a Silvia Nappini,^c Elena Magnano.^{c,d}

* The author to whom correspondence should be addressed: cherk@surface.tu-darmstadt.de

Experimental details

The polycrystalline LCP-LCPO thin films with average thicknesses of 700 nm were grown on Pt substrates by using radio-frequency (RF) sputtering of LiCoPO_4 as a target material. The choice of Pt collector was made due to chemical inertness of noble metals to oxidation during the film growth. The base pressure in the ultrahigh vacuum (UHV) chamber before the film deposition was $p_{\text{base}} \sim 5 \times 10^{-9}$ mbar (see the details of the setup in ref. ¹⁵). The films were deposited at room temperature in argon (Ar) atmosphere ($p_{\text{Ar}} \approx 1 \times 10^{-2}$ mbar) and afterwards they were annealed at 700° C in air. The annealing was carried out by using a laser heating setup.²⁵ *In-situ* photoelectron spectroscopy (XPS and UPS) experiments on the pristine LCP-LCPO film materials were carried out in the Darmstadt Integrated System for Battery Research (DAISY-BAT) by using a PHI 5000 VersaProbe spectrometer (Physical Electronics) with $p_{\text{base}} < 5 \times 10^{-9}$ mbar and the Darmstadt Integrated System for Fundamental Research (DAISY-FUN) equipped with PHOIBOS 150 spectrometer (SPECS Surface Nano Analysis GmbH) with $p_{\text{base}} < 5 \times 10^{-10}$ mbar. Monochromatic Al $K\alpha$ ($h\nu=1486.7$ eV), He I

($h\nu=21.2$ eV) and He II ($h\nu=40.8$ eV) photon sources were used in the DAISY-BAT and DAISY-FUN.

The quasi *in-situ* synchrotron photoelectron emission experiments were carried out at BESSY II (Berlin) and Elettra (Trieste). *BESSY synchrotron facilities:* The soft XPS and O K- XANES were carried out at the U56-2/PGM-1 undulator beamline with a plane grating monochromator with an accessible energy range of 60-1300 eV on the Solid Liquid Interface Analysis (SoliAS) endstation equipped with a SPECS PHOIBOS 150 MCD-9 electron analyzer.³⁵ *Elettra synchrotron facilities:* The soft XPS, O K-, P L- XANES were carried out on BACH elliptically polarized undulator beamline with a spherical grating monochromator, which allows an accessible energy range of 35-1600 eV.⁴⁵ The BACH endstation is equipped with VG-Scienta R3000 hemispherical analyser.⁵⁵ The binding energies of the photoemission spectra were referenced to the Fermi level of a clean Au- or Ag- polycrystalline foils with the energy resolution better than 300 meV and 150 meV for photon energies below 400 eV, as well as around 600 meV and 300 meV for photon energy of 1000 eV for BESSY II and Elettra, respectively. The synchrotron photoemission experiments were carried out by selecting suitable photon energies in order to collect photoelectrons with defined kinetic energies, E_{kin} , thereby providing the same analysis depth for all core level- and valence- electrons. The depth resolved photoemission experiments were carried out by varying the relevant kinetic energies. The probing depth was estimated from $d=3 \lambda(E_{kin})\cos\theta$, where λ is the electron's inelastic mean free path (IMFP) according to the TPP – 2M equation.⁶⁵ θ is the electron emission angle with respect to the surface normal. Three different emission angles ($\theta=0^\circ$, 45° and 60°) were used to probe different depth of the samples. Accordingly, a maximal surface sensitivity and a lowest surface sensitivity of the photoemission experiments corresponded to $\lambda \sim 6 \text{ \AA}$ and $\lambda \sim 35 \text{ \AA}$, respectively. The XANES were performed in total

electron yield mode (TEY) at BESSY II and Elettra giving the probing depth of about 100 Å.⁷⁵ The partial electron yield (PEY) mode was used at BESSY II to collect electrons from the depth of ≤ 30 Å.⁸⁵ The work function of LCP-LCPO films was estimated from the secondary electron cut-off measured with $h\nu=21.2$ eV, $h\nu=47$ eV, $h\nu=200$ eV and $h\nu=1486.7$ eV. The pristine LCP-LCPO thin film cathode materials grown in Darmstadt were delivered to SoliAS and/or to BACH beamline by using a transferable UHV chamber (DAISY-MOVE) equipped with a nonevaporable getter (NEG) pump, which maintains a pressure below 10^{-9} mbar.

The electrochemical experiments were carried out by using a Swagelok-type two electrode cell. 1M LiPF₆ in 4:1 wt/wt Dimethyl Carbonate (DMC): Fluorinated Ethylene Carbonate (FEC) + 0.2%wt Trimethylboroxine (TMB) (Solvionic) was used as an electrolyte. A metallic lithium foil was used as anode and Celgard®2500 as separator. *The experiments at BESSY II:* After soft XPS and XANES of pristine LCP-LCPO, the film material was transported in Ar-atmosphere to a glovebox (MBraun) for assembling the LCP-LCPO battery cell followed by its charging to a certain potential in the 3.1 – 5.1 V range (Gamry Instrument, Interface 1000 TM). The current vs time characteristics was recorded until a steady state was reached under a certain charging potential. The cell was then disassembled, the LCP-LCPO film was rinsed in DMC, dried in Ar-atmosphere and transported under Argon to SoliAS for the further photoemission and XANES experiments. *The experiments at Elettra:* The LCP-LCPO films were electrochemically charged to 4.85 V, 4.92 V and 5.1 V in Darmstadt by using cyclic voltammetry (a VMP2 potentiostat, Princeton Applied Research, USA) with the 0.1 mV/s scan rate. The charged and rinsed LCP-LCPO films were transported in Ar-atmosphere to Elettra. By connecting the DAISY-MOVE (containing the pristine samples) and transferable chamber (containing the charged samples) to the BACH station, the LCP-LCPO films were transferred to the analysis chamber (p_{base} below 4×10^{-10} mbar). At the end of synchrotron

experiments, the LCP-LCPO films were transported under vacuum conditions for the XRD analysis. Structural characterization was carried out in a parallel beam configuration using an X-ray diffractometer with Cu $K\alpha$ radiation (Rigaku SmartLab, 9 kW).

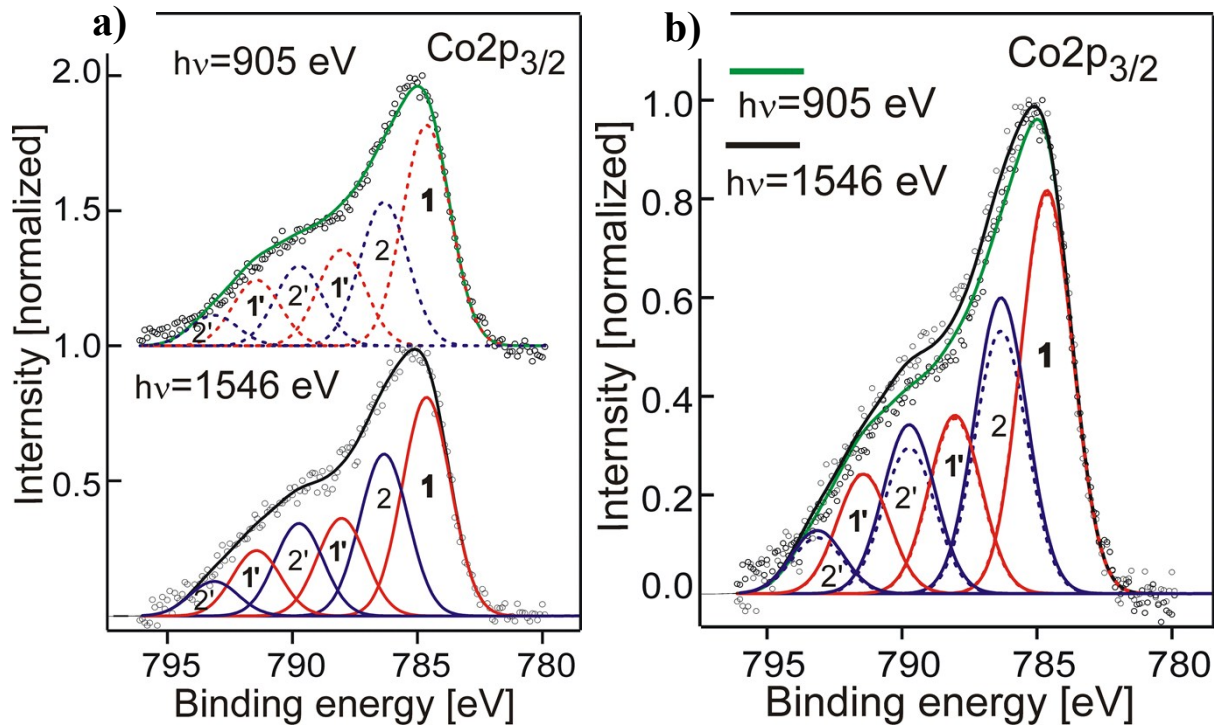


Figure S1. Supplementary Information: **a)** The $\text{Co}2p_{3/2}$ photoemission of a LCP-LCPO thin film cathode material measured at $h\nu=1546$ eV (bottom) and $h\nu=905$ eV (top), giving the probing depth of $d\sim 70$ Å and $d\sim 20$ Å, respectively. The $\text{Co}2p_{3/2}$ photoelectron spectra are normalized to the maximal intensity and spectrally decomposed into components ascribed to the two different phosphate phases followed by the fitting of the spectra. The spectral features 1, 1' and 2, 2' belong to LiCoPO_4 and $\text{LiCo}_2\text{P}_3\text{O}_{10}$, respectively. 1 and 2 are the well screened $2p^53d^8\bar{L}$ final state. 1' and 2' are the poorly screened mixture of $2p^53d^7$ and $2p^53d^9\bar{L}^2$ final states; \bar{L} and \bar{L}^2 are one and two holes in the $\text{O}2p$ band (see ref. 2S for the details). **b)** The normalized $\text{Co}2p_{3/2}$ photoemission measured at the two different energy excitations are plotted together. The relative change of the spectral features related to olivine (1, 1') and tripolyphosphate (2, 2') versus the probing depth are shown by solid and dash lines.

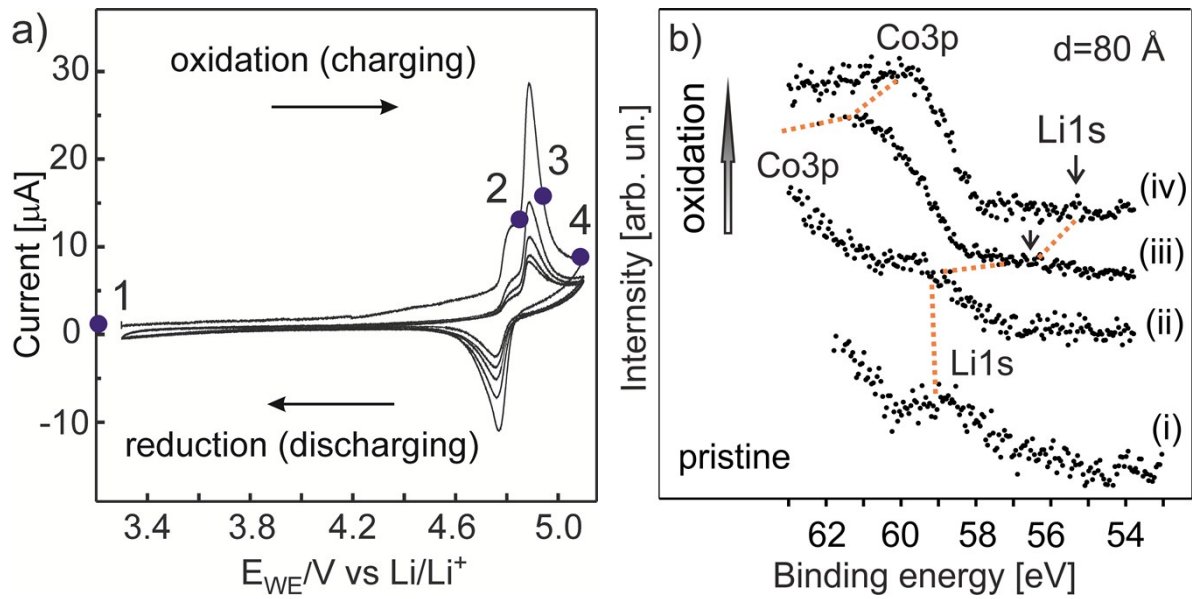


Figure S2. Supplementary Information: (a) Cyclic voltammogram (CV) of the carbon free tailored LCP-LCPO thin film (~ 700 nm thickness) positive electrode material. The closed circles denote the electrochemical steps: (1) the open circuit voltage, $ocv = 2.9$ V; (2-4) 4.83 V, 4.91 V and 5.05 V charging states, respectively. (b) The evolution of the Li1s photoemission ($h\nu = 1100$ eV) versus a charging potential (steps 2 - 4 in **Figure S2a**). The dashed line shows the position of the Li1s and Co3p photoemissions vs the electrochemical steps. The shift of the Li1s photoemission towards high binding energy at the 4.83 V charging potential (ii) is a consequence of the double layer formation at the contact to electrolyte (OCV, step 1 in **Figure S2a**). The observed shift of the Li1s and Co3p photoelectron spectra towards lower binding energies agree with the expected downward shift of the E_F level induced by the Li^+ vacancies in delithiated cathode material. The Li1s photoelectron emission attenuates with the increasing charging potential and vanishes completely at 5.1 V. The vertical arrows show the binding energy position of the Li1s photoemission at a high charging potential 4.91 V (iii) and 5.05 V (iv). In fully delithiated LCP-LCPO (denoted as \square CP- \square CPO (iv)), the virtual position of the Li1s binding energy is estimated from the relevant core levels photoemission.

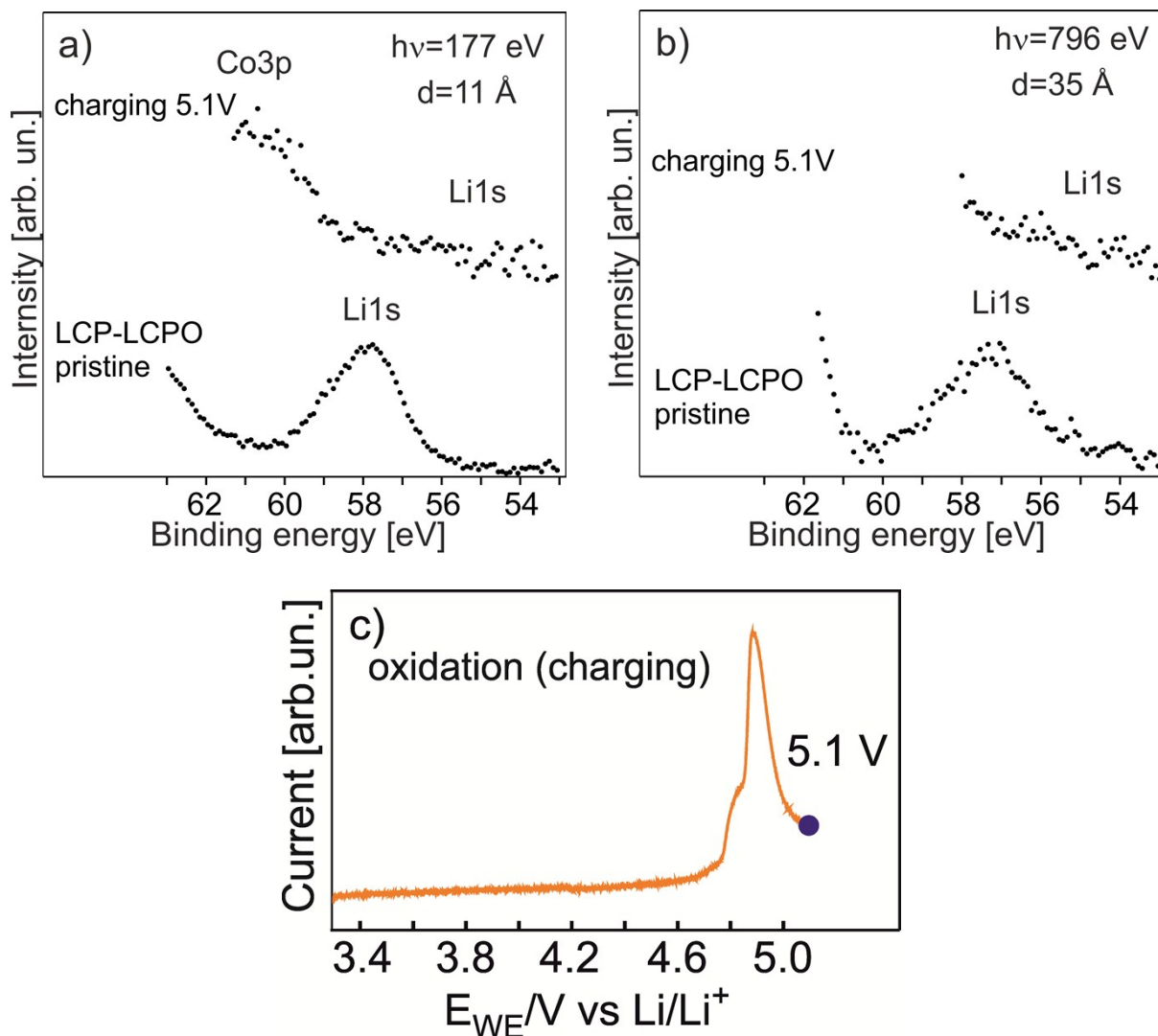


Figure S3. Supplementary Information: The $\text{Li}1s$ photoemission of the tailored LCP-LCPO thin film (pristine and charged to 5.1 V) yielded from the different depths, $d=11 \text{ \AA}$ (a) and $d=35 \text{ \AA}$ (b). No lithium is detected on the analyzed depths at the 5.1 V charging state, thereby evidencing fully delithiated LCP-LCPO (denoted as $\square\text{CP}-\square\text{CPO}$). The cyclic voltammetry curve of the LCP-LCPO film (c) was measured up to the 5.1 V charging state (denoted as a solid blue circle). Afterward, the LCP-LCPO film was rinsed in DMC under Ar-atmosphere and used for the photoemission experiments (the upper spectra in **Figure S3 (a,b)**).

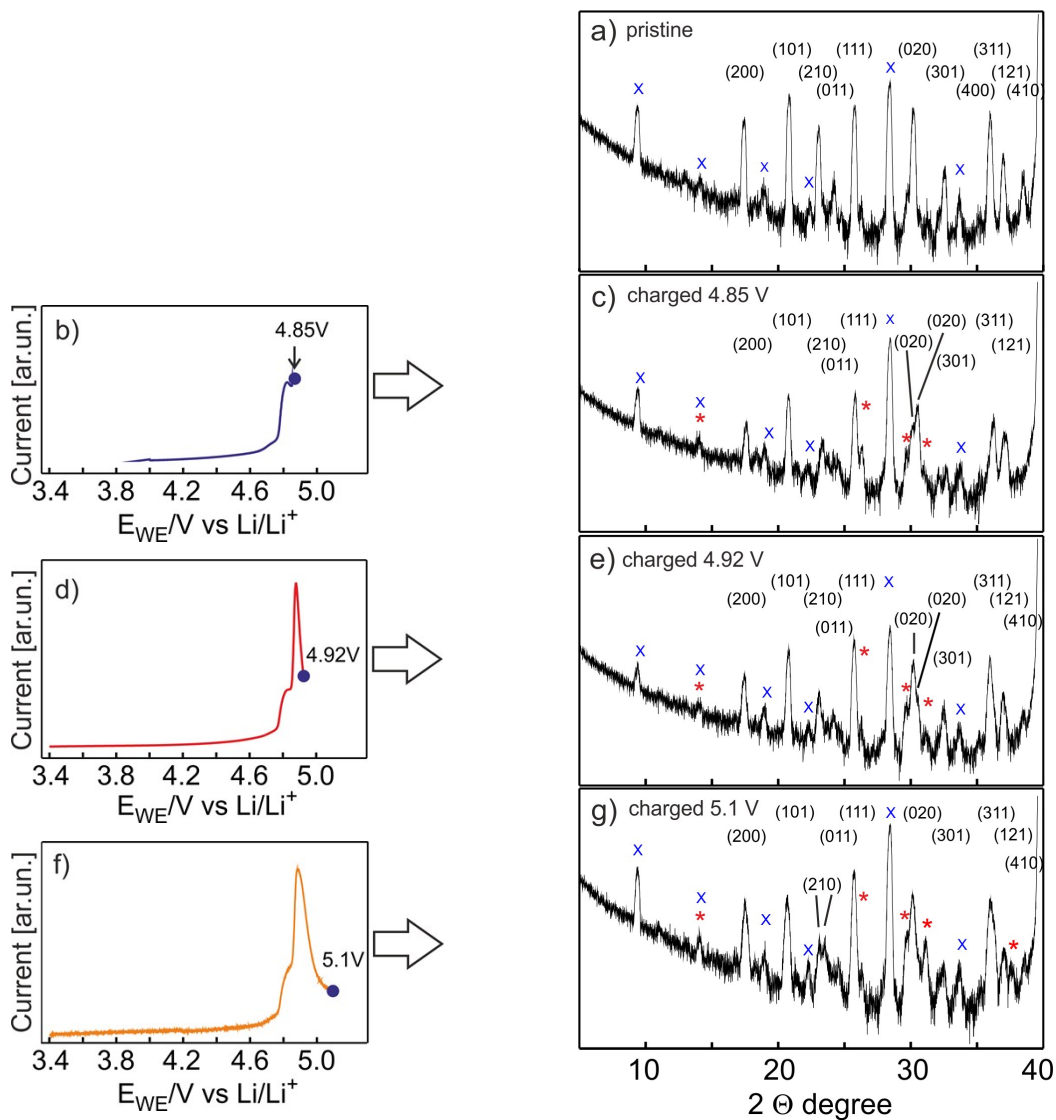


Figure S4. The cyclic voltammograms (on the left) at a charging state of 4.85V (b), 4.92V (d) and 5.1V (e) denoted as a solid blue circle and the relevant XRD patterns (on the right). a) XRD pattern of as-prepared LCP-LCPO tailored thin film material ($T=750^\circ C$) indexed to olivine $LiCoPO_4$ of $Pnma$ space group symmetry (the ICSD No. 01-078-5576). The second phase crystallographic phase ($LiCo_2P_3O_{10}$) of $P2_1/m(11)$ space group symmetry (the ICSD No. 04-011-4098) is shown by cross (X); (c, e, g) XRD of LCP-LCPO tailored thin films ($T=700^\circ C$) at a charging state of 4.85 V (c), 4.92 V (e) and 5.1 V (g). Olivine structure ($CoPO_4$) and $Co_2PO_3O_{10}$ both are preserved in fully delithiated tailored material (denoted as $\square CP-\square CPO$). The transition to the $Co(PO_3)_2$ phase (the ICSD No. 00-027-1120) of $I^*/a(15C)$ space group symmetry in delithiated LCP-LCPO takes also place (shown by stars (*)).

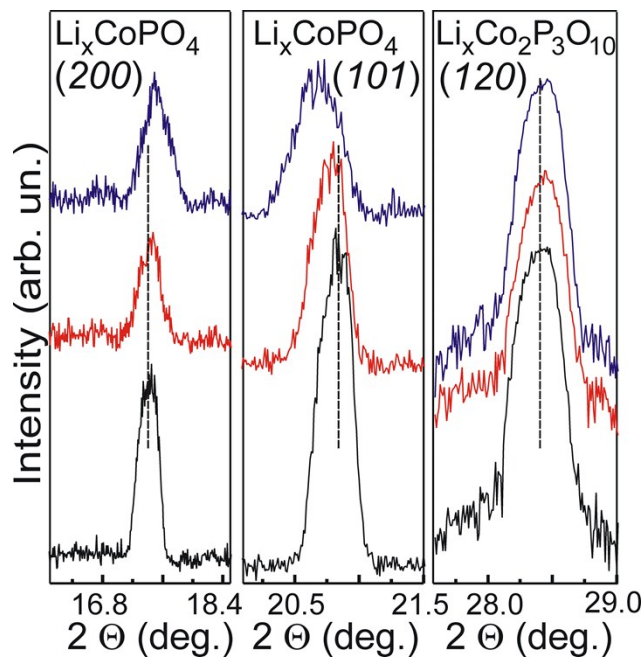


Figure S5. The variation of the XRD reflexes of olivine phase (200), (101) and dicobalt triphosphate (120) in the tailored LCP-LCPO thin film material under a charging potential: pristine (black); 4.92 V (red) and 5.1V (blue). The $(n,l,0)$ and (n,l,c) reflexes are shifted to the opposite directions with delithiation due to shrinking and extension of (a,b) and (c) cell parameters, respectively, in accordance with the previous studies on LCP.⁹⁵ The highest intensity (120) reflex at $2\theta = 28.4^\circ$, pertaining to dicobalt triphosphate, does not disappear in the fully delithiated material, but its half-width is slightly increased with a very minor the peak position shift (by $\sim 0.02^\circ$) to higher θ values.

The analysis of the shift in the XRD peak positions under delithiation of LCP-LCPO thin film (**Figure S5**) evidences that the (200) peak maximum of the olivine phase shifts by approximately 0.2° to a higher 2θ when the cathode material is charged to a potential of 5.1 V, in agreement with the previous studies.^{95,105} The broadening of the peak and the associated asymmetry evidences the occurrence of delithiated olivine phase. On the other hand, the (101) reflection was found to shift simultaneously to lower 2θ when LCP-LCPO is charged to a potential of 5.1 V. This indicates that, while the ' a ' lattice parameter (200) of Li_xCoPO_4 reduces upon lithium removal, the ' c ' lattice increases concurrently, contributing to

the observed expansion of interplanar spacing of the (101) peaks, which is in agreement with the lattice parameters obtained by Rietveld refinement.⁹⁵ This suggests an anisotropic volume compression up on lithium removal assuming that, the structure (*Pnma*, $\square\text{CoPO}_4$) remains unchanged. Additionally, there was only minor shifts observed in the position of the $\square\text{Co}_2\text{P}_3\text{O}_{10}$ (120) peak (+0.3° at 5.1 V) for which theoretical and experimental considerations for delithiation are not yet reported.

For the detailed study of the atomic arrangement associated with olivine and tripolyphosphate phases, HRTEM and STEM techniques could be useful to resolve the atomic sized interface between two phases. These experiments are planning to perform in the nearest future.

References to Supporting Information

- 1S G. Cherkashinin, D. Enslin and W. Jaegermann, *J. Mater. Chem. A*, 2014, **2**, 3571.
- 2S a) G. Cherkashinin, S. U. Sharath and W. Jaegermann, *Adv. Energy Mater.*, 2017, **7**, 1602321; b) G. Cherkashinin, presented at LiBD-8, Arcachon, France, 11-16 June, 2017; c) G. Cherkashinin, presented at EMN 3CG Workshop on Crystal Growth for Renewable Energy and Energy Storage, Berlin, Germany, 7-11 August, 2017.
- 3S Th. Mayer, M. Lebedev, R. Hunger and W. Jaegermann, *Appl. Surf. Sci.*, 2005, **252**, 31.
- 4S M. Zangrando, M. Finazzi, G. Paolucci, G. Comelli, B. Diviacco, R. P. Walker, D. Cocco and F. Parmigiani, *Rev. Sci. Instrum.*, 2001, **72**, 1313.
- 5S G. Drera, G. Salvinelli, J. Åhlund, P. G. Karlsson, B. Wannberg, E. Magnano, S. Nappini and L. Sangaletti, *J. Electron Spectroscopy Relat. Phenom.*, 2014, **195**, 109.
- 6S a) S. Tanuma, C. J. Powell and D. R. Penn, *Surf. Interface Analys.*, 1993, **21**, 165; b) C. J. Powell and A. Jablonski, *NIST Electron Inelastic-Mean-Free-Path Database*,

Version 1.2, SDR 71; National Institute of Standards and Technology, Gaithersburg, MD, 2010.

- 7S M. Abbate, J. B. Goedkoop, F. M. F. de Groot, M. Grionit, J. C. Fuggle, S. Hofmann, H. Petersen and M. Sacchi, *Surf. Interface Anal.* 1992, **18**, 65.
- 8S G. Cherkashinin, M. Motzko, N. Schulz, T. Späth and W. Jaegermann, *Chem. Mater.*, 2015, **27**, 2875.
- 9S M. Kaus, I. Issac, R. Heinzmann, S. Doyle, S. Mangold, H. Hahn, V. S. K. Chakravadhanula, C. Kübel, H. Ehrenberg and S. Indris, *J. Phys. Chem. C*, 2014, **118**, 17279.
- 10S M. G. Palmer, J. T.; Frith, A. L. Hector, A. W. Lodge, J. R. Owen, C. Nicklin and J. Rawle, *Chem. Commun.*, 2016, **52**, 14169.